cMyb regulates hematopoietic stem/progenitor cell mobilization during zebrafish hematopoiesis

*Yiyue Zhang,[1] *Hao Jin,[1] Li Li,[1] F. Xiao-Feng Qin,[2] and Zilong Wen[1]

[1]State Key Laboratory of Molecular Neuroscience, Division of Life Science, The Hong Kong University of Science and Technology, Hong Kong, People's Republic of China; and [2]Laboratory of Cellular and Molecular Immunobiology, School of Life Sciences, Sun Yat-sen University, Guangzhou, People's Republic of China

The establishment of the HSC pool in vertebrates depends not only on the formation and the propagation of these stem cells but also on their proper trafficking among the defined hematopoietic organs. However, the physiologic mechanisms that regulate HSC mobilization remain elusive. Through analysis of the zebrafish *cmyb* mutant *cmyb*^{hkz3}, we show that the suppression of cMyb function abrogates larval and adult hematopoiesis, with concomitant accumulation of hematopoietic stem/progenitor cells (HSPCs) in their birthplace, the ventral wall of the dorsal aorta (VDA). Cell tracking and time-lapse recording reveal that the accumulation of HSPCs in *cmyb*^{hkz3} mutants is caused by the impairment of HSPC egression from the VDA. Further analysis demonstrates that the HSPC migratory defects in *cmyb*^{hkz3} mutants are at least partly because of adversely elevated levels of chemokine stromal cell-derived factor 1a (Sdf1a). Our study reveals that cMyb plays a hitherto unidentified role in dictating physiologic HSPC migration by modulating Sdf1a signaling. (*Blood*. 2011;118(15):4093-4101)

Introduction

In vertebrates, hematopoiesis is a dynamic process that occurs in several successive waves.[1,2] In mice, the primitive wave is initiated in the extra embryonic yolk sac and mainly generates embryonic erythrocytes and macrophages. This is followed by the definitive wave, which can continuously give rise to all blood lineages during fetal life and adulthood.[1,2] Sustained multilineage blood production through definitive hematopoiesis relies on the existence of self-renewing common progenitors termed HSCs that reside in discrete anatomical sites during development.

It is now widely accepted that HSCs originate from the endothelium in the aorta-gonad-mesonephros (AGM) region,[3-7] although the placenta[8,9] and the yolk sac[10] may also have the potential to form HSCs. These AGM-derived HSCs are believed to colonize the fetal liver (FL) and ultimately the BM,[2,11] where they replicate and differentiate to replenish the supply of peripheral blood cells throughout fetal and adult life.[1,2] This pathway is evolutionarily conserved from teleost fish to humans.[11] In zebrafish, hematopoietic stem/progenitor cells (HSPCs) arise from the endothelium in the ventral wall of the dorsal aorta (VDA), a mammalian AGM counterpart, at around 30 hours post fertilization (hpf).[4,5] Through in vivo fate mapping, these VDA-derived HSPCs have been shown to migrate to an intermediate hematopoietic compartment, the posterior blood island (PBI) or caudal hematopoietic tissue (CHT), before colonizing the kidney, the definitive hematopoietic organ in adult fish.[12-15] Thus, the VDA, the CHT, and the kidney are the functional analogues of the mammalian AGM, FL, and BM, respectively. However, despite the delineation of the HSPC colonization pathway, the mechanisms that control HSPC mobilization from their birthplace to the downstream hematopoietic organs remain unclear.

The transcription factor cMyb was initially identified as a proto-oncogene associated with the development of avian leukemia.[16] Studies on hematopoietic cell lines have shown that the expression of cMyb is largely restricted to HSCs and progenitor cells and is down-regulated on differentiation.[17,18] Various cMyb mutant mouse alleles have been developed to investigate the physiologic functions of cMyb, and they have revealed that cMyb plays important roles in many hematopoietic pathways, including lymphoid development, HSPC maintenance, and HSPC differentiation.[19-27] In particular, cMyb-null mice failed to develop fetal liver hematopoiesis and did not live past the embryonic stage. The cause generally ascribed to diminished fetal liver hematopoiesis in cMyb-null mice is impaired HSPC proliferation/differentiation in the absence of an intact cMyb gene.[16] Recently, *cmyb* zebrafish and medaka mutants have been identified that display similar phenotypes: failure of definitive hematopoiesis in the larval and adult stages.[28,29] However, it is unclear whether cMyb also plays an earlier role in regulating HSPC development in the AGM or the VDA in these animals.

In this article, we report a previously unknown function of *cmyb* in definitive hematopoiesis using a *cmyb*^{hkz3} zebrafish mutant line isolated from our *N*-ethyl-*N*-nitrosourea (ENU) mutant collection. This mutant harbors a splice mutation that results in the synthesis of a truncated cMyb protein lacking its transactivation domain.[30] In *cmyb*^{hkz3} mutants, definitive hematopoiesis is initiated normally in the VDA but is compromised in the larval and the adult hematopoietic organs. Unexpectedly, we found that excessive HSPCs accumulated in the VDA of

Submitted March 12, 2011; accepted August 3, 2011. Prepublished online as *Blood* First Edition paper, August 19, 2011; DOI 10.1182/blood-2011-03-342501.

The online version of this article contains a data supplement.

The publication costs of this article were defrayed in part by page charge payment. Therefore, and solely to indicate this fact, this article is hereby marked "advertisement" in accordance with 18 USC section 1734.

*Y.Z. and H.J. contributed equally to this work.

cmyb^{hkz3} mutants, and that this is a result of the impairment of HSPC egression from the VDA. We further show that impaired HSPC egression from the VDA is caused by adversely up-regulated expression of chemokine stromal cell-derived factor 1a (Sdf1a) in *cmyb*^{hkz3} mutants. These findings suggest that, in addition to its previously known functions, cMyb also plays a role in mobilizing HSPCs from their site of initiation by down-regulating Sdf1a retention signaling.

Methods

Fish line

Zebrafish were raised as described previously.[31,32] The following fish strains were used in this study: AB, WIK, Tg(*cd41*:eGFP),[33] Tg(*gata1*:DsRed),[34] Tg(*flk1*:eGFP).[35]

Laser-activated cell labeling

Lineage tracking was performed as described previously.[15] Briefly, the DMNB caged-Flu alone or along with morpholino was injected into 1-cell-stage embryos from cmyb$^{hkz3/+}$Tg(*cd41*:eGFP) intercrosses. Subsequently, cells—irrespective of Cd41-eGFP expression—along the aortic floor were uncaged through focusing and confining 405-nm laser excitation to a defined segment of the aortic floor.

WISH

Antisense digoxigenin (DIG)–labeled RNA probes were generated by in vitro transcription and whole-mount in situ hybridization (WISH) was performed according to "the zebrafish book."[32]

Double staining for *cmyb* or *sdf1a* RNA and eGFP protein

To detect *cmyb* or *sdf1a* RNA and eGFP protein simultaneously, RNA was first developed with cy3-tyramide and protein was subsequently detected using Abs as described.[15]

IHC analysis

The procedure for double Ab staining using eGFP/Flu and eGFP/αE1-globin has been described previously.[15] For eGFP and DsRed costaining, embryos were incubated with goat-anti-eGFP Ab (abcam) and rabbit-anti-DsRed Ab (clontech) and visualized using Alexa Fluor 488 donkey anti–goat and Alexa Fluor 555 donkey anti–rabbit (Invitrogen), respectively.

Morpholino injection

For knockdown experiments, 1-cell-stage embryos were injected with 2 nL of *sdf1a* morpholino (5′-CTACTACGATCACTTTGAGATCCAT-3′) at a concentration of 1mM as reported.[36]

Cell proliferation assay

Embryos at 54 hpf were incubated in 10mM BrdU (Sigma-Aldrich) for 2 hours and fixed for IHC as described with minor modifications.[37] The embryos were stained with mouse-anti-BrdU (Roche) and goat-anti-eGFP Abs (Abcam), followed by Alexa Fluor 555 anti–mouse (Invitrogen) and Alexa 488 anti–goat (Invitrogen) for fluorescent visualization.

Cell sorting and live cell-cycle analysis

For cell sorting, *cmyb*^{hkz3}/Tg(*cd41*:eGFP) mutant embryos were separated from their siblings under an epifluorescence microscope based on the fact that there was marked accumulation of CD41-eGFP^{+} cells in the VDA of mutants. Cell suspensions were prepared from the trunk tissue dissected from ~ 200 *cmyb*^{hkz3}/Tg(*cd41*:eGFP) embryos or siblings as described.[38] Other tissues were collected for confirmation by genotyping. Genotyping was done by sequencing the PCR-amplified DNA fragment using the following genotyping primers: 5′-TTGCACCTTATCACACCACA A-3′/5′-GGAGAAAGAAACTCAAGTGAAAGG-3′. FACS and live cell cycle analysis were performed as described.[38,39] For sorting, a 70-μm nozzle was used for allowing cells to pass through in a FACS Aria II flow cytometer (Becton Dickinson). For detecting Hoechst and eGFP signal, near UV laser and 488nm laser were used, respectively.

Quantitative RT-PCR

Total RNA from sorted cells and embryos was extracted using the RNeasy Kit (QIAGEN). For cDNA preparation from the total RNA of embryos, RT was performed using Omniscript RT Kit (QIAGEN). For specific detection of *cmyb* WT or *hkz3* aberrant splicing form, the following primer sets were used: the common forward primer is 5′-CACTGCTGCTATCCAGAGA-CACTAC-3′ (814_FP), and the reverse primers are 5′-AGCCGTTCATG-GAGATTGGTAG-3′ (947_wt_RP) and 5′-CATGGAGATCTGGGTG-GGGG-3′ (947_hkz3_RP) specific for *cmyb* WT form and *hkz3* aberrent splicing form, respectively. The primer set for indiscriminately detecting both *cmyb* forms is 5′-GCACGAGAAACTTGGAAACCGATG-3′/5′-GCTTGGTGTGTGATTGTAGTTC-3′ (575_FP/782_wt_RP). For preparation of cDNA from total RNA of sorted cells, SuperScript III first-strand synthesis system (Invitrogen) was used. Primers of β-*actin* and hematopoietic and endothelium markers were described,[13] whereas the primer set of *sdf1a*is5′-TTCCAAGTCATTGCCAAACTG-3′/5′-GGCTGTCAGATTTCCTT-GTC-3′.

Time-lapse recordings

The Tg(*cd41*:eGFP) and *cmyb*^{hkz3}/Tg(*cd41*:eGFP) embryos were stained with Bodipy TR (Invitrogen) and mounted with 3% methylcellulose on 35-mm glass-bottom dishes for imaging on an inverted confocal microscope (Olympus) as described.[40] The Tg(*cd41*:eGFP) embryos with overexpression of *sdf1a* plus *mCherry* or *mCherry* alone were mounted with 3% methyl cellulose for imaging.

Genetic screening and positional cloning

ENU mutagenesis was carried out as described previously.[39] *cmyb*^{hkz3} mutant was identified because of its complete absence of *lysozyme C* (*lyz*) expression. Linkage scanning was done with bulky segregation analysis guided by the Zon laboratory's positional cloning instruction (http://zon.tchlab.org/). Intermediate resolution mapping with 39 embryos localized *cmyb*^{hkz3} mutation 23.08cM south to z20039 and 1.28cM north to z5141 on linkage group 23. *cmyb* gene was mapped to this genetic interval. Mutation in *cmyb* genomic locus was identified through sequencing.

Transactivation assay

To construct the yeast expression vectors for the GAL4 fusion proteins, the wild-type and *hkz3* mutated cMyb TAD fragments were cloned into the 2 hybrid bait plasmid pGBKT7 (Clontech). The yeast strain AH109 (Clontech) was used for the yeast growth inhibition experiment.

Establishment of the Tg(*hsp70:*Myc-cMyb) line and rescue of *cmyb*^{hkz3} mutants

For generation of the Tg(*hsp70:*myc-cMyb) transgenic line, zebrafish heat shock protein (*hsp*) 70 promoter driving the Myc-tagged *cmyb* was inserted into pToL vector with minimal Tol2 elements and a SV40 polyA sequence. One-cell stage *cmyb*^{hkz3}/Tg(*cd41*:eGFP) embryos were injected with this construct together with Tol2 transposase mRNA and raised to adult. The founder fish was identified by PCR. The stable F1 Tg(*hsp70:*myc-cMyb) embryos were obtained by mating founder fish with AB and confirmed by anti-Myc immunostaining. For Myc-cMyb Ab staining, 35-hpf Tg(*hsp70*:myc-cMyb) embryos were heat-shocked at 40°C for 1 hour and recovered at 28°C for 2 hours before fixed for anti-Myc Ab staining. For cMyb rescue experiment, *cmyb*^{hkz3}/Tg(*cd41*:eGFP)/Tg(*hsp70*:myc-cMyb) embryos and siblings were heat-shocked at 40°C at 28, 35, and 48 hpf for 1 hour and fixed at 53 hpf for anti-eGFP staining to detect Cd41-eGFP^{+} cells.

Sdf1a transient overexpression experiment

For transient overexpression of *sdf1a*, 1-cell-stage Tg(*cd41*:eGFP) embryos were injected with CMV:*sdf1a* construct together with CMV:*mCherry* construct which expressed Sdf1a and mCherry from a constitutively active CMV promoter. Embryos injected with CMV:*mCherry* were used as negative controls.

Statistical analysis

Statistical evaluation was performed by using the 2-tailed *t* test. Differences were considered significant if the *P* value was $< .05$.

Results

Failure of larval and adult definitive hematopoiesis in the *cmyb*^{hkz3} zebrafish mutant line.

To investigate the molecular basis of HSPC formation, trafficking, maintenance, and differentiation, we took advantage of a zebrafish *cmyb* mutant line (*cmyb*^{hkz3}) isolated from our ENU mutant collection. The *cmyb*^{hkz3} mutant harbors a splice mutation (supplemental Figure 1A-B, available on the *Blood* Web site; see the Supplemental Materials link at the top of the online article) that leads to the synthesis of a truncated cMyb protein lacking its transactivation domain (supplemental Figure 1C).[30] As the wild-type (WT) *cmyb* transcript was not detected in *cmyb*^{hkz3} mutants (supplemental Figure 2A) and the truncated cMyb^{hkz3} protein was inactive in a yeast transactivation assay (supplemental Figure 2B), we believe that *cmyb*^{hkz3} is a loss-of-function mutation. To characterize the effects of the *cmyb*^{hkz3} mutation on definitive hematopoiesis, we examined the expression of a panel of HSPC and lineage-specific markers in *cmyb*^{hkz3} mutant embryos at 4-5 dpf, when definitive hematopoiesis is normally well under way in the CHT, thymus and pronephros.[41] In siblings, strong *cmyb* expression, indicative of HSPCs, was found in the CHT, thymus, and pronephros (supplemental Figure 3A,C). However, in *cmyb*^{hkz3} mutants, *cmyb* expression decreased from 2 dpf onward (supplemental Figure 3E-F), and almost no *cmyb* signals were present at 4 dpf (supplemental Figure 3B,D). In the same time window, the expression of another HSPC marker, Cd41-eGFP,[40] also decreased in the CHT of *cmyb*^{hkz3} mutants (supplemental Figure 3G-H). Expression of the lymphoid marker *rag1* was absent in the developing thymus (supplemental Figure 3I), and the populations of definitive erythroid and myeloid cells, represented by *ae1-globin*[41] and *mpx*[41] RNA expression, respectively, were also profoundly decreased in *cmyb*^{hkz3} mutants (supplemental Figure 3J,K). These results demonstrate that, as in cMyb-null mice[16] and the *cmyb*^{t25127} zebrafish mutant,[29] the *cmyb*^{hkz3} mutation compromises the development of multiple blood cell lineages in definitive hematopoiesis. Presumably as a result of this large-scale failure of definitive hematopoiesis, *cmyb*^{hkz3} mutants were unable to survive to adulthood, most died around 10 dpf.

The overall phenotypic resemblance between *cmyb*^{hkz3} mutants and cMyb null mice suggests that they share common underlying cellular defects. In light of the impaired HSPC proliferation observed in the fetal liver of cMyb null mice,[16] we speculated that HSPC proliferation in the CHT of *cmyb*^{hkz3} mutants may also be hindered. To test this, we performed a BrdU incorporation assay in which *cmyb*^{hkz3}/Tg(*cd41*:eGFP) mutant embryos were pulse-labeled using BrdU at 54 hpf and then costained for eGFP and BrdU. Quantification of the eGFP/BrdU double-positive cell population in mutants and siblings showed that a decreased proportion of Cd41-eGFP$^+$ HSPCs in the CHT region of mutants incorporated BrdU (supplemental Figure 4A), suggesting that HSPC proliferation is attenuated in the CHT region of *cmyb*^{hkz3} mutants. Living cell-cycle analysis using Hoechst 33 342 staining further confirmed that the proliferation of Cd41-eGFP$^+$ precursors in 3-dpf *cmyb*^{hkz3} mutants was reduced, with a decreased proportion of cells in the S phase of the cell cycle (supplemental Figure 4B). Thus, akin to the cMyb null mutation in mice, the *cmyb*^{hkz3} mutation interrupts definitive hematopoiesis partly by impairing HSPCs proliferation in the CHT.

Accumulation of HSPCs in the VDA region of *cmyb*^{hkz3} mutants

To investigate whether there are any earlier hematopoietic defects in *cmyb*^{hkz3} mutants, we examined HSPC development in the VDA, where they are formed. Cd41 has recently been shown to be one of the earliest surface markers expressed by nascent HSPCs, appearing shortly after their emergence in the VDA.[40] Therefore, the *cmyb*^{hkz3}/Tg(*cd41*:eGFP) transgenic line was used for the analysis of HSPC development in the VDA. Surprisingly, we found that *cmyb*^{hkz3} mutant embryos had far more Cd41-eGFP positive (Cd41-eGFP$^+$) cells in their VDA than siblings from 2 dpf onward (Figure 1A, supplemental Figure 5A). The number of cells expressing *cmyb*, another HSPC marker, was similarly increased in the VDA of *cmyb*^{hkz3} mutants, and double staining with endogenous *cmyb* RNA and Cd41-eGFP showed that the majority of Cd41-eGFP$^+$ cells also stained positive for *cmyb* (Figure 1A, supplemental Figure 5B). Quantification analysis showed that *cmyb*^{hkz3} mutant embryos contained approximately twice as many *cmyb*$^+$/Cd41-eGFP$^+$ cells as their siblings from 2 dpf onward (Figure 1B). Quantitative PCR analysis further showed that *runx1* and other endothelial and HSPC markers were also increased in *cmyb*^{hkz3} embryos (Figure 1C). These results demonstrate that in *cmyb*^{hkz3} mutants, cells positive for HSPC markers accumulate in the VDA after the offstage at which definitive hematopoiesis normally begins. It is unlikely that the excess of HSPCs in the VDA is caused by the malformation of the vascular system, because double staining using αE1-globin protein and Flk1-eGFP showed intact vasculature containing well-circulating erythrocytes in *cmyb*^{hkz3} mutants (supplemental Figure 5C). The accumulation of Cd41-eGFP$^+$ cells can be reverted by reintroduction of WT *cmyb* expression, further demonstrating that this phenotype is caused by the loss of *cmyb* function (supplemental Figure 6).

To confirm that the Cd41-eGFP$^+$ cells accumulated in the VDA of *cmyb*^{hkz3} mutants are HSPCs, not differentiated cells committed to downstream lineages, we tested whether there was a concomitant increase in the differentiated lineage markers *gata1* and *mpx*, indicative of erythroid and myeloid cells, respectively, in the VDA of *cmyb*^{hkz3} mutants. Imaging of 52 hpf *cmyb*^{hkz3}/Tg(*gata1*:DsRed)/Tg(*cd41*:eGFP) mutant embryos and their siblings revealed that gata1-DsRed–positive cells did not accumulate as Cd41-eGFP$^+$ cells did in mutant embryos (supplemental Figure 7A). Similarly, no obvious increase in myeloid cell populations was found in the *cmyb*^{hkz3} mutant VDA as shown by the normal *mpx* staining (supplemental Figure 7B). Taken together, the increased expression of HSPC markers but not differentiated lineage markers strongly indicates that the Cd41-eGFP$^+$ cells accumulated in the *cmyb*^{hkz3} mutant VDA are HSPCs. This was further supported by video-enhanced differential interference contrast (DIC) imaging analysis,[42] which showed that the accumulated Cd41-eGFP$^+$ cells in *cmyb*^{hkz3} mutant embryos had large nuclei and little cytoplasm, morphologic features identical to those of HSPCs described previously (supplemental Figure 7C).[40]

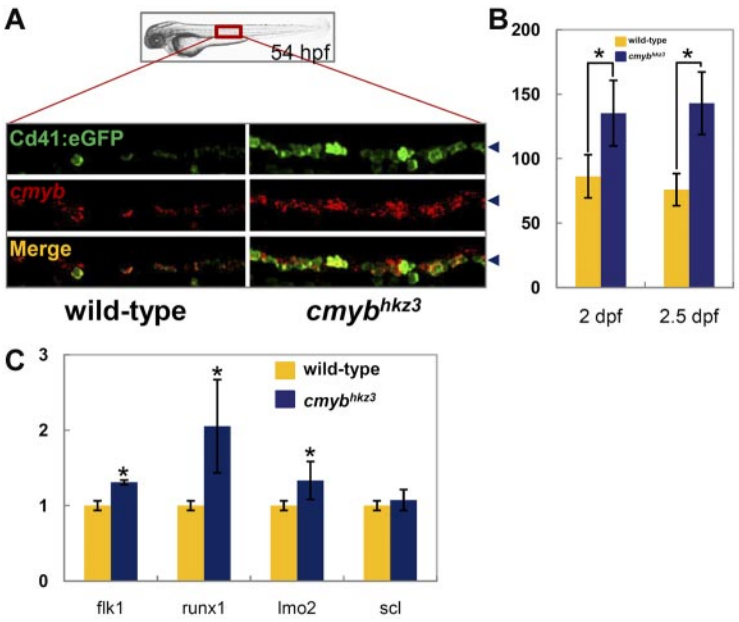

Figure 1. Accumulation of HSPCs in the VDA of *cmyb*^{hkz3} mutants. (A-B) Excessive Cd41-eGFP^{+} cells accumulated in the VDA of *cmyb*^{hkz3} mutants. Double staining of Cd41:eGFP protein (top panel) and *cmyb* RNA (middle panel) in 54-hpf siblings (left panel) and *cmyb*^{hkz3} mutant embryos (right panel) of *cmyb*^{hkz3}/Tg(*cd41*:eGFP) transgenic lines (A). The bottom panel shows merged images. Blue arrowheads in panel A indicate the signal position in the VDA region. Quantification of Cd41-eGFP–positive cells in the VDA region in siblings (yellow columns) and *cmyb*^{hkz3} mutant embryos (blue columns) of *cmyb*^{hkz3}/Tg(*cd41*:eGFP) transgenic lines at 2 dpf (left columns) and 2.5 dpf (right columns; B). Units on the y-axis represent eGFP-positive cell numbers ($n \geq 5$, mean ± SD). Asterisks indicate statistical difference with corresponding sibling (*t* test, $P < .05$). (C) Quantitative RT-PCR of expression of endothelium and HSPC specific genes in trunk of wild-type (yellow columns) and *cmyb*^{hkz3} embryos (blue columns) at 2 dpf. Expression level was normalized with *β-actin* expression.

The accumulation of HSPCs in *cmyb*^{hkz3} mutants is because of the impairment of HSPC egression from the VDA

In principle, HSPC accumulation in the VDA of *cmyb*^{hkz3} mutants could result from any one or more of the 3 following underlying cellular abnormalities: (1) augmented de novo HSPC genesis in the VDA; (2) enhanced proliferation of existing VDA HSPCs; (3) impaired HSPC egression from the VDA. To determine whether HSPCs are generated in excess in *cmyb*^{hkz3} mutant embryos, we monitored the expression of the early HSPC marker *runx1* at 30 hpf, when HSPCs are normally transiting from the endothelium and no HSPCs are released from the VDA into circulation.[13,14,40] The results showed that neither the number of *runx1*$^{+}$ cells nor the per-cell expression level of *runx1* was changed in *cmyb*^{hkz3} mutants, indicating that the hemogenic aortic endothelial cells competent to transform into HSPCs are formed normally in *cmyb*^{hkz3} mutants (Figure 2A-B).

We next investigated the proliferation of the accumulated VDA Cd41-eGFP^{+} cells in *cmyb*^{hkz3} mutants using a BrdU pulse-labeling experiment (Figure 2C). Quantification of the Cd41-eGFP/BrdU double positive cell population showed that Cd41-eGFP^{+} HSPCs in the VDA of *cmyb*^{hkz3} mutants and siblings incorporated BrdU comparably (Figure 2D), indicating that HSPC proliferation in the VDA is not affected by *cmyb*^{hkz3} mutation.

The above observations suggest that the accumulation of HSPCs in *cmyb*^{hkz3} mutants is caused by the impairment of HSPC egression from the VDA. To prove that HSPC migration is defective in *cmyb*^{hkz3} mutants, we tracked the migration of HSPCs from the VDA to the CHT using a photoactivatable tracer, DMNB-caged fluorescein (Flu).[15] In this assay, cells in the aortic floor were labeled at 30 hpf by exposing embryos injected with DMNB-caged Flu to a 405-nm laser pulse and Cd41-eGFP/Flu double-positive cells in the CHT were scored 16 hours later (Figure

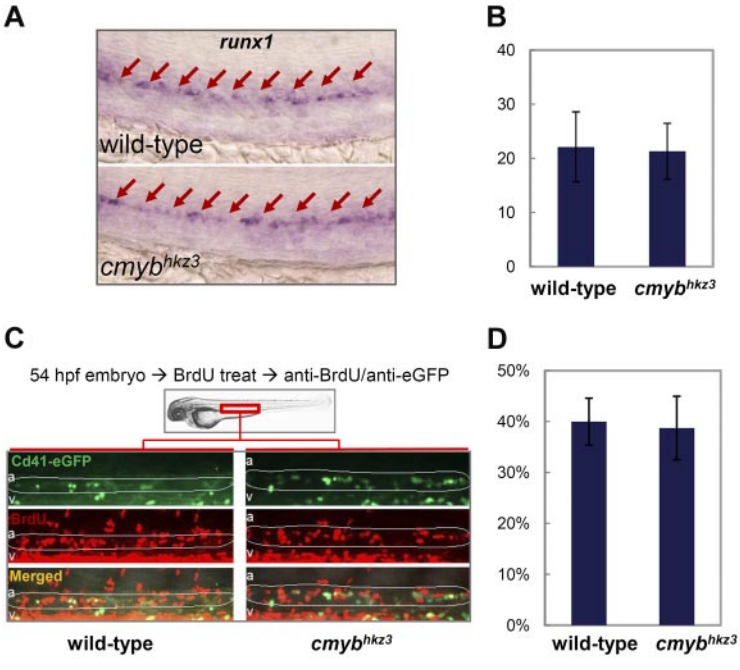

Figure 2. Accumulation of Cd41-eGFP^{+} HSPCs in *cmyb*^{hkz3} mutants is not caused by enhanced HSPC formation or proliferation. (A) WISH of *runx1* expression in the VDA region in the 30-hpf sibling (top panel) and *cmyb*^{hkz3} mutant (bottom panel) embryos. Arrows identify *runx1*-positive cells in the VDA. (B) Counts of *runx1*-positive cell in 30-hpf sibling and *cmyb*^{hkz3} mutant embryos ($n \geq 6$, mean ± SD). (C) Profiling of BrdU incorporation by VDA Cd41-eGFP^{+} cells in *cmyb*^{hkz3}/Tg(*cd41*:eGFP) mutants and their siblings by double staining of BrdU and cd41:eGFP. Green indicates eGFP; red, BrdU; a, aorta; and v, vein. Circled (white) regions are the VDA regions. (D) Statistical data showing the percentage of VDA localized Cd41^{+} HSPCs that incorporate BrdU ($n \geq 7$, mean ± SD).

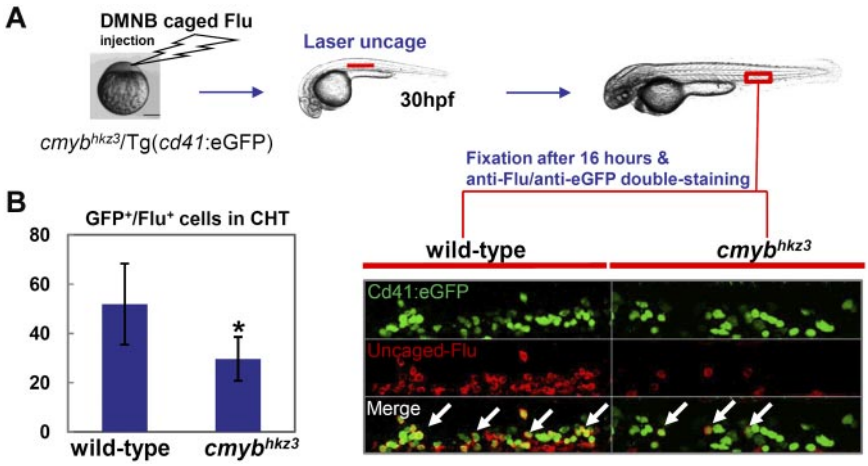

Figure 3. VDA-derived Cd41-eGFP$^+$ HSPCs are impaired in populating the CHT in *cmyb*^{hkz3} mutants. (A) The *cmyb*^{hkz3}/Tg(*cd41*:eGFP) embryos were injected with DMNB-caged Flu at 1-cell stage. The aortic floor, where Cd41-eGFP$^+$ HSPCs will later derive, was labeled by exposure to a pulse flash of UV at 30 hpf. (B) Emergence of eGFP/Flu double-positive cells (right panel, white arrows indicated) were scored and quantified in the CHT 16 hours after UV exposure (left panel). Representative figure was shown in the right panel (eGFP, green; uncaged-Flu, red). Units on the y-axis represent the average number of eGFP/Flu double-positive cells ($n \geq 9$, mean $\pm$ SD). An asterisk indicates significant difference with sibling (*t* test, $P < .05$).

3A). Counting the number of Cd41-eGFP/Flu double-positive cells in the CHT disclosed that, compared with siblings, the amounts of VDA-derived HSPCs in the CHT of mutants were markedly reduced (Figure 3). The migrated Cd41-eGFP$^+$ cells in *cmyb*^{hkz3} mutant embryos only amounted to approximately half of those in siblings (Figure 3B), suggesting that navigation of HSPCs from the VDA to the CHT was impaired by the *cmyb*^{hkz3} mutation. Notably, when we prolonged the chasing period after uncaging from 10 hours to 24 hours, we observed a further decrease in the number of Cd41-eGFP/Flu double-positive cells in the CHT of these prolonged chased *cmyb*^{hkz3} mutants (supplemental Figure 8). As mutant HSPCs in the CHT were impaired in the proliferation (supplemental Figure 4), the further reduction of VDA derived HSPCs in the CHT of *cmyb*^{hkz3} mutants after prolonged chasing period likely reflects the manifestation of this proliferative defect in mutants tracked for a longer period of time (supplemental Figure 4).

To directly demonstrate that the HSPC defects result from the crippled egression of HSPCs from the VDA, as opposed to defects in mobility after egression, live imaging analysis with *cmyb*^{hkz3}/Tg(*cd41*:eGFP) embryos was used to measure the frequency of Cd41-eGFP$^+$ HSPCs release from the VDA between 50 hpf and 60 hpf, a time period in which HSPCs normally migrate from the VDA to the CHT.[15,40] Time-lapse fluorescence confocal microscopy of sibling embryos during this time period showed that Cd41-eGFP$^+$ cells often changed their shape from round to elongated and vice versa, and some of them entered the vein lumen, rolling along vein walls toward the anterior or disappearing in circulation (Figure 4A, supplemental Video 1), as has been previously reported.[40] In *cmyb*^{hkz3} mutant embryos at equivalent developmental stages, the movements of Cd41-eGFP$^+$ cells were similar, but very few Cd41-eGFP$^+$ cells were released from the VDA (Figure 4B, supplemental Video 2). Quantification analysis revealed that during the first 2 hours of observation, 4 cells left from the VDA in a representative sibling embryo, compared with only 1 in a *cmyb*^{hkz3} mutant (Figure 4A-C, supplemental Videos 1-2). At 4.5 hours, 9 cells were released from the VDA in the sibling, compared with only 3 cells did so in the *cmyb*^{hkz3} mutant (Figure 4A-C, supplemental Videos 1-2). Interestingly, VDA-trapped Cd41-eGFP HSPCs in *cmyb*^{hkz3} mutants became much brighter than WT Cd41-eGFP HSPCs during recording. This is possibly because of their longer time spent in the VDA as it has been reported that the fluorescence levels of Cd41-eGFP HSPCs increase after the cells emerge from the aortic floor.[40] The quantitative difference between *cmyb*^{hkz3} mutants and siblings in the number of HSPCs released

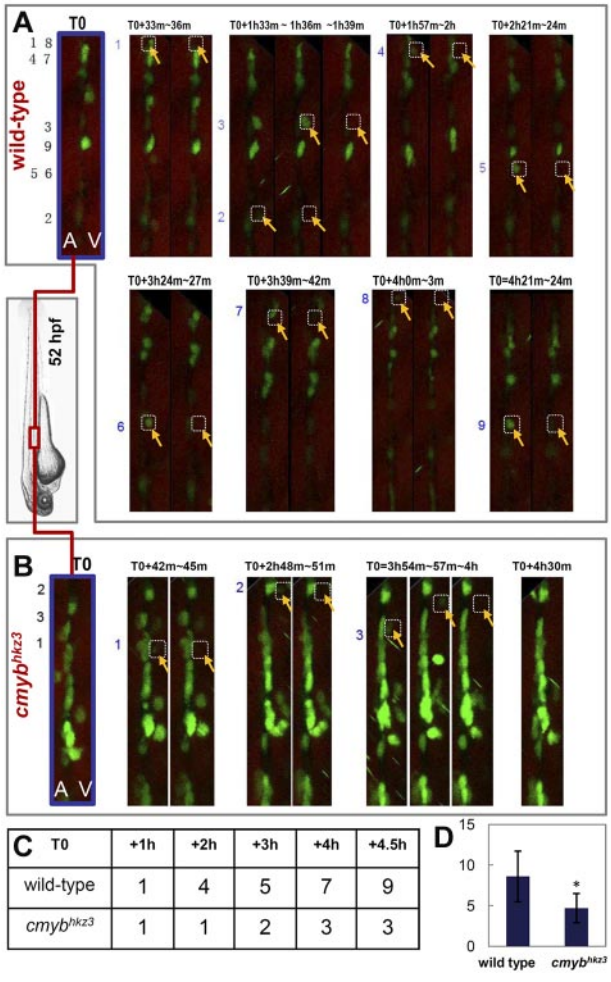

C T0	+1h	+2h	+3h	+4h	+4.5h
wild-type	1	4	5	7	9
cmyb^{hkz3}	1	1	2	3	3

Figure 4. Accumulation of Cd41-eGFP$^+$ HSPCs in *cmyb*^{hkz3} mutants results from crippled egress of HSPCs from the VDA. (A-B) Still image sequence extracted from confocal microscopic recording of red boxed VDA area in *cmyb*^{hkz3}/Tg(*cd41*:eGFP) mutant embryo (B) and sibling (A) between 50 and 60 hpf in each 3-minute interval. Corresponding movies for panels A and B are shown in supplemental Videos 1 and 2, respectively. T0 is the still confocal image taken at the beginning of imaging with black number indicating cells eventually undergoing egress within the recording period. Numbered HSPCs (yellow arrows) were released into circulation at time points indicated above each panel. A, aorta; V, vein. (C) A corresponding summary of the sequence of cells exiting from the VDA in sibling (A) and *cmyb*^{hkz3} mutant (B). (D) Quantification of the numbers of Cd41-eGFP$^+$ HSPCs exiting from the VDA in a 5-hour recording period in 2- to 2.5-hpf embryos ($n = 5$, mean $\pm$ SD). An asterisk indicates significant difference with wild type (*t* test, $P < .05$).

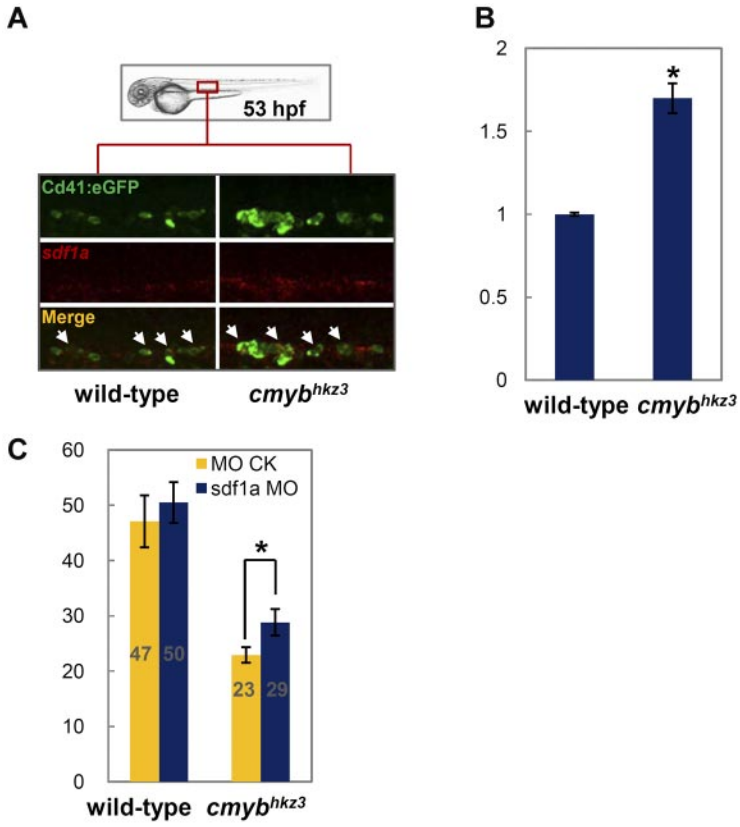

Figure 5. cMyb regulates HSPC migration through modulating Sdf1a level. (A) Double staining of Cd41:eGFP protein (top panel) and *sdf1a* RNA (middle panels) in 53-hpf siblings (left panel) and *cmyb*^{hkz3} mutant embryos (right panel) of *cmyb*^{hkz3}/Tg(*cd41*:eGFP) (representative figures). The bottom panels show merged images. (B) Quantitative RT-PCR for *sdf1a* gene expression in purified Cd41-eGFP$^+$ cells from the VDA region of *cmyb*^{hkz3}/Tg(*cd41*:eGFP) mutants and siblings. Units on the y-axis represent the relative fold change of *sdf1a* expression in siblings and *cmyb*^{hkz3} mutant embryos. Expression level was normalized with *β-actin* expression. Error bars, SD. (C) HSPC migratory defect in *cmyb*^{hkz3} was rescued by *sdf1a* MO knockdown. *cmyb*^{hkz3}/Tg(*cd41*:eGFP) mutant and sibling embryos were injected with *sdf1a* MO plus DMNB-caged Flu (blue columns) or control MO plus DMNB-caged Flu (yellow columns) at 1-cell stage and cells in the aortic floor were then labeled through photoactivation. Emergence of eGFP/Flu double-positive cells in the CHT (gray numbers in each column) were scored and quantified 16 hours after photoactivation. Units on the y-axis represent the average number of eGFP/Flu double-positive cell per embryo ($n \geq 19$, mean ± SE). An asterisk indicates a statistics significant increase of the number of eGFP/Flu double-positive cells migrated to the CHT in *cmyb*^{hkz3} mutants injected with *sdf1a* MO compared with *cmyb*^{hkz3} mutants injected with control MO (*t* test, $P < .05$).

from VDA is roughly in agreement with the uncaging result, which estimated a 2-fold reduction in the number of VDA-derived HSPCs colonizing the CHT in *cmyb*^{hkz3} mutant embryos (Figure 3B, supplemental Figure 8, and Figure 4D). Together, photoactivated cell tracing and live imaging analysis demonstrate that impaired HSPC migration is one of the major reasons for the accumulation of HSPCs in the VDA of *cmyb*^{hkz3} mutants, and that this accounts at least in part for the diminished larval hematopoiesis observed in the secondary hematopoietic organs of these embryos.

The cMyb-Sdf1a axis plays an essential role in the regulation of HSPC migration

Chemokine signaling has been shown to be an important pathway for directing cell migrations, such as primordial germ cell migration, during embryogenesis and HSPCs mobilization in adulthood.[36,43] In particular, several studies in mammals have indicated that the down-regulation of the chemokine stromal cell-derived factor 1 (SDF1), which is normally constitutively expressed in the BM and cells such as CD34$^+$ progenitor cells,[44] is tightly associated with G-CSF–induced HSPC mobilization from the BM into the peripheral blood.[45] We therefore postulated that chemokine signaling may play a role in cMyb-mediated HSPC egression from the VDA. To test this possibility, we examined the expression of several key molecules involved in chemokine signaling in *cmyb*^{hkz3} mutants and siblings. We found that, in 53-hpf WT embryos, *sdf1a* transcripts were faintly detected and were costained with the majority of Cd41-eGFP$^+$ cells (Figure 5A). Notably, in *cmyb*^{hkz3} mutants, *sdf1a* expression was found to be moderately up-regulated in VDA Cd41-eGFP$^+$ cells. Consistently, RT-PCR analysis of Cd41-eGFP$^+$ cells sorted from the dissected trunk regions of 2-dpf embryos showed that *sdf1a* expression was markedly increased in *cmyb*^{hkz3} mutants compared with siblings (Figure 5B). As high concentrations of sdf1 have been documented to act as a retention signal for HSCs in the BM of mice, we reasoned that the abnormally high levels of Sdf1a in *cmyb*^{hkz3} mutants may trap HSPCs in the VDA. To test this hypothesis, 2 assays were carried out. We first reduced Sdf1a levels using antisense morpholino (MO) knockdown to see whether this could rescue the migratory defects of HSPCs in *cmyb*^{hkz3} mutants. Photoactivated cell tracing analysis showed that in *cmyb*^{hkz3} mutants receiving *sdf1a*-MO, the number of VDA-born HSPCs seeding the CHT increased 26% compared with embryos receiving control MO (Figure 5C). No obvious difference was seen in control siblings injected with *sdf1a*-MO and control MO (Figure 5C). We then assayed whether ectopically elevating Sdf1a level in HSPCs in WT embryos was sufficient to trap HSPCs in the VDA. This was achieved by comparing the emigration of CD41-eGFP$^+$ HSPCs from the VDA of embryos mosaicly overexpressing Sdf1a plus mCherry and mCherry alone. Live imaging revealed that Cd41-eGFP$^+$ HSPCs with Sdf1a ectopic expression tend to remain in the VDA for longer periods of time compared with Cd41-eGFP$^+$ HSPCs in the same embryos without Sdf1a overexpression and those with only mCherry overexpression (Figure 6A-B; supplemental Videos 3-4). Quantitatively, only 27% of Cd41-eGFP/mCherry double-positive HSPCs in Sdf1a overexpressed embryos exited the VDA region within 9 hours, whereas 57% of these cells in control embryos did within the same recording period (Figure 6C). Taken together, these data demonstrate that the defective egression of HSPCs from the VDA in *cmyb*^{hkz3} mutants is at least partly because of the adverse elevation of Sdf1a expression in HSPCs, indicating that cMyb-mediated attenuation of *sdf1a* expression is required for HSPC release from the VDA.

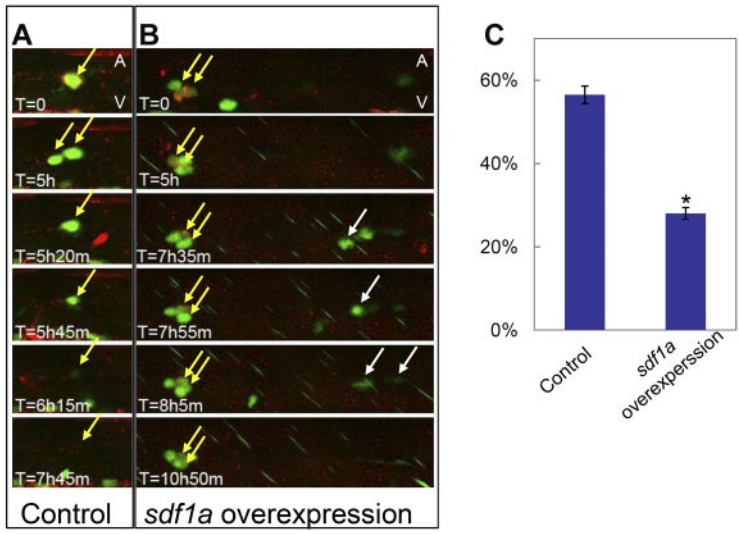

Figure 6. *Sdf1a* overexpression can retain HSPCs in the VDA. (A-B) Still image sequences extracted from time-lapse confocal microscopic recording of the VDA region of Tg(*cd41*:eGFP) embryos mosaicly expressing mCherry alone (A control) and mCherry plus *Sdf1a* (B *Sdf1a* overexpression). The corresponding videos were shown in supplemental Video 3 (control) and supplemental Video 4 (*Sdf1a* overexpression). Yellow arrows identify the VDA localized Cd41-eGFP$^+$/mCherry$^+$ HSPCs that are trapped in *Sdf1a* overexpression embryos (B) but released in control embryos (A). Of note, in *Sdf1a* overexpression embryos (B), Cd41-eGFP$^+$ HSPCs without *Sdf1a* overexpression were also released from the VDA (white arrows). (C) Quantification of the percentage of exited Cd41-eGFP$^+$/mCherry$^+$ cells in Tg(*cd41*:eGFP) embryos mosaicly overexpressing *mCherry* plus *sdf1a* (*Sdf1a* overexpression) and *mCherry* alone (control) in a 12-hour recording ($n \geq 19$, mean $\pm$ SD). An asterisk indicates a statistical differences with embryos mosaicly overexpressing *mCherry* alone (*t* test, $P < .05$).

Discussion

In this study, we isolated a novel *cmyb* zebrafish mutant allele, *cmyb*^{hkz3}, failed to undergo definitive hematopoiesis in the CHT, kidney, and thymus, akin to the phenotypes of cMyb-null mice and zebrafish *cmyb*^{t25127}.[16,29] Strikingly, we observed that HSPCs in *cmyb*^{hkz3} mutants accumulated in their birthplace, the VDA, as a result of the diminished egression of HSPCs from the VDA to the CHT. Thus, the migratory defects of HSPCs are likely to be the earliest factor leading to the failure of fetal/larval and adult hematopoiesis in cMyb-deficient animals. Beyond 2 dpf in the CHT, the gradual reduction of the expression of *cmyb* and Cd41-eGFP, 2 definitive HSPC markers, could be observed more and more clearly. However, *cmyb* expression decreased more dramatically in the CHT at 4 dpf than Cd41-eGFP expression. As thrombocytes display high Cd41-eGFP expression[40] and the CHT-born erythromyeloid progenitors (EMPs)[46] also expressed Cd41-eGFP, the residual Cd41-eGFP expression in the CHT of mutants might reflect the presence of circulating thrombocytes and EMP or EMP-derived cells that were preserved in *cmyb*^{hkz3} mutants. Nonetheless, tracing the VDA-derived Cd41-eGFP$^+$ cells to the CHT shows consistent reduction in *cmyb*^{hkz3} mutants during the normal time window of HSPC migration, demonstrating a bona fide role of *cmyb* in controlling HSPC migration.

Notably, while *cmyb*^{hkz3} mutants show only a 2-fold reduction in HSPC migration from the VDA to the CHT, the reduction in the populations of further differentiated blood cells in the CHT, kidney, and thymus past 4 dpf is much more profound. This is likely because of the proliferation defect of mutant HSPCs in these subsequent hematopoietic compartments shown by cell-cycle and cell-tracking analysis, which is consistent with the observation in c-Myb null mice.[16] As cMyb is also known to be required for T-cell development in mice[23]; the complete absence of thymic *rag1* expression in *cmyb*^{hkz3} mutants might be caused by a combination of reduction of definitive hematopoietic precursors and blockage of T-cell development. Thus, we believe that the profound decrease in multilineage hematopoiesis in definitive organs likely reflects the disruption of the functions of *cmyb* in multiple aspects of hematopoietic development. Through analysis of the *cmyb*^{hkz3} mutant, our study reveals that cMyb plays a role in regulating the exit of HSPCs from their birthplace, the VDA, for the colonization of the larval hematopoietic organ, the CHT, a function which has not been found in previous studies of *cMyb*-deficient models. To our knowledge, cMyb is the first clue to the molecular control of the earliest step of the developmental trafficking of HSPCs during ontogeny. However, the question of whether *cmyb* also regulates HSPC intravasation from the CHT remains unclear, and this would be an interesting topic for future study.

Mechanistically, we show that the cMyb-regulated HSPC mobilization is mediated at least in part by suppressing the expression of *sdf1a*, a chemokine molecule in HSPCs. In this model, nascent HSPCs should express a relatively high level of *sdf1a*, which serves as a brake to prevent the precocious release of HSPCs from the VDA. As HSPCs mature, *sdf1a* expression in HSPCs is down-regulated by cMyb, and this facilitates HSPC release from the VDA. This is consistent with previous observations in mice showing that the down-regulation of SDF1 is tightly associated with G-CSF–induced HSPC mobilization from the BM into the peripheral blood.[45] Notably, in mammals, SDF-1 is constitutively expressed by stromal cells in the BM and CD34$^+$ progenitor cells.[44] Our study shows that Sdf1a expressed by HSPCs contributes to the regulation of HSPC mobilization from the VDA to the CHT. However, the contribution of relevant stromal cells to local Sdf1a levels in the VDA and to HSPC mobilization remains unexplored because of lack of knowledge of stromal elements in the VDA region. The question of whether *sdf1a* is a direct or indirect target of cMyb is currently unclear and requires future study.

The SDF1-CXCR4 axis plays a role in HSC migration in mammals.[47] We have attempted to address the involvement of candidate *sdf1a* receptors, *cxcr4a* and *cxcr4b*,[48] in mediating cMyb regulated HSPC mobilization. However, unlike *sdf1a* expression, which is up-regulated, the expression of *cxcr4a/4b* is unaffected in the HSPCs of *cmyb*^{hkz3} mutants (data not shown), suggesting that *cmyb* may control the expression of the ligand rather than the receptor to modulate chemokine signaling. However, the administration of CXCR4 antagonist AMD3100[49] failed to rescue the HSPC mobilization defects in *cmyb*^{hkz3} mutants (data not shown), a result that could be because of either inefficient penetration and targeting of the compound or the fact that Sdf1a uses different receptors in the VDA. Thus, cognate receptors and downstream transducers that mediate Sdf1a signaling in the context of HSPC mobilization from the VDA to the CHT remain to be identified and characterized in future studies.

The characterization of cMyb as a physiologic regulator of HSPC trafficking may have pathologic implications. It is known that aberrant cMyb activity is associated with the development of a variety of human cancers, including leukemia, lymphomas, colon carcinomas, and melanoma,[50] presumably via up-regulating tumor cell growth.[51] On the other hand, cancer stem cells also express the SDF1 receptor CXCR4 on their surfaces, and the SDF1-CXCR4 axis has been implicated in the direction of metastasis.[52] Our new findings suggest that cancer cells may hijack the cMYB-SDF1 axis for their metastasis. In light of this, it may prove useful to investigate the role of cMYB and its interaction with the SDF1 chemokine signaling pathway in tumorgenesis.

Acknowledgments

The authors thank V. Korzh, R. Handin, L. Zon, and P. Herbomel for providing *sdf1a* probe, Tg(*cd41*:eGFP), Tg(*gata1*:DsRed) transgenic fish, and DIC system advice, respectively. They thank Anthony Zhang for editing the manuscript.

This work was supported by the Area of Excellence Scheme established under the University Grants Committee of the Hong Kong Special Administration Region (HKSAR; grant AoE/B-15/01) and by the General Research Fund (GRF) grants from the Research Grants Council of the HKSAR (grant 662808; grant 663109).

Authorship

Contribution: Y.Z., H.J., and L.L. designed the research, performed experiments, and analyzed data; F.X.-F.Q and Z.W. designed the research and analyzed data; and Y.Z., H.J., and Z.W. participated in the preparation of manuscript.

Conflict-of-interest disclosure: The authors declare no competing financial interests.

Correspondence: Zilong Wen, State Key Laboratory of Molecular Neuroscience, Division of Life Science, The Hong Kong University of Science and Technology, Clear Water Bay, Kowloon, Hong Kong, People's Republic of China; e-mail: zilong@ust.hk.

References

1. Mikkola HK, Orkin SH. The journey of developing hematopoietic stem cells. *Development.* 2006; 133(19):3733-3744.
2. Cumano A, Godin I. Ontogeny of the hematopoietic system. *Annu Rev Immunol.* 2007;25:745-785.
3. Medvinsky A, Dzierzak E. Definitive hematopoiesis is autonomously initiated by the AGM region. *Cell.* 1996;86(6):897-906.
4. Boisset JC, van Cappellen W, Andrieu-Soler C, Galjart N, Dzierzak E, Robin C. In vivo imaging of haematopoietic cells emerging from the mouse aortic endothelium. *Nature.* 2010;464(7285):116-120.
5. Kissa K, Herbomel P. Blood stem cells emerge from aortic endothelium by a novel type of cell transition. *Nature.* 2010;464(7285):112-115.
6. Bertrand JY, Chi NC, Santoso B, Teng S, Stainier DY, Traver D. Haematopoietic stem cells derive directly from aortic endothelium during development. *Nature.* 2010;464(7285):108-111.
7. Muller AM, Medvinsky A, Strouboulis J, Grosveld F, Dzierzak E. Development of hematopoietic stem cell activity in the mouse embryo. *Immunity.* 1994;1(4):291-301.
8. Gekas C, Dieterlen-Lievre F, Orkin SH, Mikkola HK. The placenta is a niche for hematopoietic stem cells. *Dev Cell.* 2005;8(3):365-375.
9. Ottersbach K, Dzierzak E. The murine placenta contains hematopoietic stem cells within the vascular labyrinth region. *Dev Cell.* 2005;8(3):377-387.
10. Samokhvalov IM, Samokhvalova NI, Nishikawa S. Cell tracing shows the contribution of the yolk sac to adult haematopoiesis. *Nature.* 2007; 446(7139):1056-1061.
11. Orkin SH, Zon LI. Hematopoiesis: an evolving paradigm for stem cell biology. *Cell.* 2008;132(4): 631-644.
12. Murayama E, Kissa K, Zapata A, et al. Tracing hematopoietic precursor migration to successive hematopoietic organs during zebrafish development. *Immunity.* 2006;25(6):963-975.
13. Burns CE, Traver D, Mayhall E, Shepard JL, Zon LI. Hematopoietic stem cell fate is established by the Notch-Runx pathway. *Genes Dev.* 2005;19(19):2331-2342.
14. Gering M, Patient R. Hedgehog signaling is required for adult blood stem cell formation in zebrafish embryos. *Dev Cell.* 2005;8(3):389-400.
15. Jin H, Xu J, Wen Z. Migratory path of definitive hematopoietic stem/progenitor cells during zebrafish development. *Blood.* 2007;109(12):5208-5214.
16. Mucenski ML, McLain K, Kier AB, et al. A functional c-myb gene is required for normal murine fetal hepatic hematopoiesis. *Cell.* 1991;65(4): 677-689.
17. Gonda TJ, Metcalf D. Expression of myb, myc and fos proto-oncogenes during the differentiation of a murine myeloid leukaemia. *Nature.* 1984;310(5974):249-251.
18. Mukai HY, Motohashi H, Ohneda O, Suzuki N, Nagano M, Yamamoto M. Transgene insertion in proximity to the c-myb gene disrupts erythroid-megakaryocytic lineage bifurcation. *Mol Cell Biol.* 2006;26(21):7953-7965.
19. Thomas MD, Kremer CS, Ravichandran KS, Rajewsky K, Bender TP. c-Myb is critical for B cell development and maintenance of follicular B cells. *Immunity.* 2005;23(3):275-286.
20. Bender TP, Kremer CS, Kraus M, Buch T, Rajewsky K. Critical functions for c-Myb at three checkpoints during thymocyte development. *Nat Immunol.* 2004;5(7):721-729.
21. Badiani P, Corbella P, Kioussis D, Marvel J, Weston K. Dominant interfering alleles define a role for c-Myb in T-cell development. *Genes Dev.* 1994;8(7):770-782.
22. Pearson R, Weston K. c-Myb regulates the proliferation of immature thymocytes following beta-selection. *EMBO J.* 2000;19(22):6112-6120.
23. Lieu YK, Kumar A, Pajerowski AG, Rogers TJ, Reddy EP. Requirement of c-myb in T cell development and in mature T cell function. *Proc Natl Acad Sci U S A.* 2004;101(41):14853-14858.
24. Xiao C, Calado DP, Galler G, et al. MiR-150 controls B cell differentiation by targeting the transcription factor c-Myb. *Cell.* 2007;131(1):146-159.
25. Garcia P, Clarke M, Vegiopoulos A, et al. Reduced c-Myb activity compromises HSCs and leads to a myeloproliferation with a novel stem cell basis. *EMBO J.* 2009;28(10):1492-1504.
26. Sandberg ML, Sutton SE, Pletcher MT, et al. c-Myb and p300 regulate hematopoietic stem cell proliferation and differentiation. *Dev Cell.* 2005; 8(2):153-166.
27. Lieu YK, Reddy EP. Conditional c-myb knockout in adult hematopoietic stem cells leads to loss of self-renewal due to impaired proliferation and accelerated differentiation. *Proc Natl Acad Sci U S A.* 2009;106(51):21689-21694.
28. Moriyama A, Inohaya K, Maruyama K, Kudo A. Bef medaka mutant reveals the essential role of c-myb in both primitive and definitive hematopoiesis. *Dev Biol.* 2010;345(2):133-143.
29. Soza-Ried C, Hess I, Netuschil N, Schorpp M, Boehm T. From the cover: essential role of c-myb in definitive hematopoiesis is evolutionarily conserved. *Proc Natl Acad Sci U S A.* 2010;107(40): 17304-17308.
30. Greig KT, Carotta S, Nutt SL. Critical roles for c-Myb in hematopoietic progenitor cells. *Semin Immunol.* 2008;20(4):247-256.
31. Kimmel CB, Ballard WW, Kimmel SR, Ullmann B, Schilling TF. Stages of embryonic development of the zebrafish. *Dev Dyn.* 1995;203(3):253-310.
32. Westerfield M. The zebrafish book. *A Guide for the Laboratory Use of Zebrafish (Danio rerio).* 4th ed. Eugene, OR: University of Oregon Press, 2000.
33. Lin HF, Traver D, Zhu H, et al. Analysis of thrombocyte development in CD41-GFP transgenic zebrafish. *Blood.* 2005;106(12):3803-3810.
34. Traver D, Paw BH, Poss KD, Penberthy WT, Lin S, Zon LI. Transplantation and in vivo imaging of multilineage engraftment in zebrafish bloodless mutants. *Nat Immunol.* 2003;4(12):1238-1246.
35. Jin SW, Beis D, Mitchell T, Chen JN, Stainier DY. Cellular and molecular analyses of vascular tube and lumen formation in zebrafish. *Development.* 2005;132(23):5199-5209.
36. Doitsidou M, Reichman-Fried M, Stebler J, et al. Guidance of primordial germ cell migration by the chemokine SDF-1. *Cell.* 2002;111(5):647-659.
37. Harris JA, Cheng AG, Cunningham LL, MacDonald G, Raible DW, Rubel EW. Neomycin-induced hair cell death and rapid regeneration in the lateral line of zebrafish (Danio rerio). *J Assoc Res Otolaryngol.* 2003;4(2):219-234.
38. Du L, Xu J, Li X, et al. Rumba and Haus3 are essential factors for the maintenance of hematopoietic stem/progenitor cells during zebrafish hematopoiesis. *Development.* 2011;138(4):619-629.
39. Liu Y, Du L, Osato M, et al. The zebrafish udu gene encodes a novel nuclear factor and is essential for primitive erythroid cell development. *Blood.* 2007;110(1):99-106.
40. Kissa K, Murayama E, Zapata A, et al. Live imaging of emerging hematopoietic stem cells and early thymus colonization. *Blood.* 2008;111(3): 1147-1156.

41. Jin H, Sood R, Xu J, et al. Definitive hematopoietic stem/progenitor cells manifest distinct differentiation output in the zebrafish VDA and PBI. *Development.* 2009;136(4):647-654.
42. Herbomel P, Thisse B, Thisse C. Ontogeny and behaviour of early macrophages in the zebrafish embryo. *Development.* 1999;126(17):3735-3745.
43. Nagasawa T, Hirota S, Tachibana K, et al. Defects of B-cell lymphopoiesis and bone-marrow myelopoiesis in mice lacking the CXC chemokine PBSF/SDF-1. *Nature.* 1996;382(6592):635-638.
44. Aiuti A, Turchetto L, Cota M, et al. Human CD34(+) cells express CXCR4 and its ligand stromal cell-derived factor-1. Implications for infection by T-cell tropic human immunodeficiency virus. *Blood.* 1999;94(1):62-73.
45. Semerad CL, Christopher MJ, Liu F, et al. G-CSF potently inhibits osteoblast activity and CXCL12 mRNA expression in the bone marrow. *Blood.* 2005;106(9):3020-3027.
46. Bertrand JY, Kim AD, Violette EP, Stachura DL, Cisson JL, Traver D. Definitive hematopoiesis initiates through a committed erythromyeloid progenitor in the zebrafish embryo. *Development.* 2007;134(23):4147-4156.
47. Petit I, Szyper-Kravitz M, Nagler A, et al. G-CSF induces stem cell mobilization by decreasing bone marrow SDF-1 and up-regulating CXCR4. *Nat Immunol.* 2002;3(7):687-694.
48. Chong SW, Emelyanov A, Gong Z, Korzh V. Expression pattern of two zebrafish genes, cxcr4a and cxcr4b. *Mech Dev.* 2001;109(2):347-354.
49. Fricker SP, Anastassov V, Cox J, et al. Characterization of the molecular pharmacology of AMD3100: a specific antagonist of the G-protein coupled chemokine receptor, CXCR4. *Biochem Pharmacol.* 2006;72(5):588-596.
50. Ramsay RG, Gonda TJ. MYB function in normal and cancer cells. *Nat Rev Cancer.* 2008;8(7):523-534.
51. Weston K. Reassessing the role of C-MYB in tumorigenesis. *Oncogene.* 1999;18(19):3034-3038.
52. Kucia M, Reca R, Miekus K, et al. Trafficking of normal stem cells and metastasis of cancer stem cells involve similar mechanisms: pivotal role of the SDF-1-CXCR4 axis. *Stem Cells.* 2005;23(7):879-894.